Wang et al. *Zool. Res. Divers. Conserv.* 2024, 1(4): 282−289
https://doi.org/10.24272/j.issn.2097-3772.2024.011
https://cstr.cn/32249.14.zrdc.2024.011

ZRDC | Zoological Research: Diversity and Conservation

Article Open Access

A new species of mountain vole (Rodentia, Cricetidae, *Neodon*) from south Xizang, China

Si-Yuan Wang[1,2,#], Yi-Xian Li[1,2,#], Quan Li[1], Wen-Yu Song[3], Hong-Jiao Wang[1], Shui-Wang He[1], Kenneth Otieno Onditi[1], Laxman Khanal[4], Xue-You Li[1], Zhong-Zheng Chen[5], Xue-Long Jiang[1,*]

[1] *Key Laboratory of Genetic Evolution and Animal Models* & *Yunnan Key Laboratory of Biodiversity and Ecological Security of Gaoligong Mountain*, *Kunming Institute of Zoology*, *Chinese Academy of Sciences*, *Kunming*, *Yunnan* 650223, *China*

[2] *Kunming College of Life Science*, *University of Chinese Academy of Sciences*; *Beijing* 100101, *China*

[3] *Vector Laboratory*, *Institute of Pathogens and Vectors*, *Yunnan Provincial Key Laboratory for Zoonosis Control and Prevention*, *Dali University*, *Dali*, *Yunnan* 671000, *China*

[4] *Central Department of Zoology*, *Institute of Science and Technology*, *Tribhuvan University*, *Kathmandu* 44618, *Nepal*

[5] *Collaborative Innovation Center of Recovery and Reconstruction of Degraded Ecosystem in Wanjiang Basin Co-founded by Anhui Province and Ministry of Education*, *School of Ecology and Environment*, *Anhui Normal University*, *Wuhu*, *Anhui* 241002, *China*

ABSTRACT

A survey of small mammals conducted on the Qinghai-Xizang Plateau in August 2023 yielded a series of specimens of a distinctive and previously unidentified *Neodon* species from high-altitude shrubland and grassland habitats at elevations of 2800–4000 m in Lhozhag County, Xizang, China. This study employed an integrative approach, combining molecular and morphological evidence to determine the taxonomic placement of the species. Results confirmed that these specimens represent a new species, formally described herein as *Neodon lhozhagensis* **sp. nov.** The new species can be distinguished from all other *Neodon* species based on larger body size, longer tail, five closed triangles in first lower molar, and obvious interorbital crest. Molecular analysis strongly supported *Neodon lhozhagensis* **sp. nov.** as a monophyletic clade that diverged from its sister taxon, *Neodon tsonaensis*, approximately 0.89–1.68 million years ago. Kimura-2-parameter genetic distances of the complete cytochrome *b* gene between *Neodon lhozhagensis* **sp. nov.** and other nominal *Neodon* species ranged from 9.3% to 12.8%. This discovery underscores the importance of continued efforts to investigate and document the biodiversity of the Himalayan region.

Keywords: *Neodon*; Small mammals; Taxonomy; Morphology; Molecular systematics

INTRODUCTION

Mountain voles of the genus *Neodon* Horsfield, 1851 (Rodentia: Cricetidae) represent a rapidly evolving group endemic to the Qinghai-Xizang Plateau and surrounding high-altitude regions. These voles exhibit high species diversity and pose an ongoing challenge in taxonomic classification (Liu et al., 2022). The genus *Neodon* was first established by Horsfield (1851), with *Neodon sikimensis* as the type species. Subsequent research throughout the 19th and 20th centuries led to the description of additional species and subspecies, as well as revisions to their taxonomic ranks based primarily on morphological traits (Corbet, 1978; Ellerman, 1941; Hinton, 1923, 1926; Horsfield, 1851; Musser & Carleton, 1993; Thomas, 1912). Advancements in molecular systematics over the past decade have prompted a reevaluation of phylogenetic relationships within *Neodon*, leading to the formal description of several new species, including *N. linzhiensis* Liu *et al*., 2012, *N. medogensis* Liu *et al*., 2017, *N. nyalamensis* Liu *et al*., 2016, *N. nepalensis* Prandhan *et al*., 2019, *N. namchabarwaensis* Liu *et al*., 2022, *N. shergylaensis* Liu *et al*., 2022, *N. liaoruii* Liu *et al*., 2022, *N. chayuensis* Liu *et al*., 2022, *N. bomiensis* Liu *et al*., 2022, *N. bershulaensis* Liu *et al*., 2022, and *N. tsonaensis* Liu, 2024. Molecular phylogenetic analyses based on multi-locus gene and genomic datasets have suggested that the diversity within *Neodon* is likely underestimated and that the genus displays substantial phylogenetic incongruences (Liu et al., 2012, 2017, 2022; Pradhan et al., 2019). Currently, 17 recognized species of *Neodon* are documented (Supplementary Table S1), most

Received: 03 October 2024; Accepted: 22 October 2024; Online: 23 October 2024

Foundation items: This work was supported by the Second Qinghai-Xizang Plateau Scientific Expedition and Research Program (2024QZKK0200, 2019QZKK05010100) and Survey of Wildlife Resources in Key Areas of Xizang (ZL202203601, ZL202303601)

[#]Authors contributed equally to this work

*Corresponding author, E-mail: jiangxl@mail.kiz.ac.cn

of which were described in recent years based on molecular evidence and morphological variations (Liu et al., 2022; Liu, 2024; Pradhan et al., 2019). Among external morphological features, the number of closed triangles in the first lower molar has proven to be a reliable taxonomic characteristic, exhibiting intraspecific stability and interspecific variation (Kryštufek & Shenbrot, 2022; Liu et al., 2012, 2017, 2022; Liu, 2024; Pradhan et al., 2019).

During a mammalian survey conducted in south Xizang, China, in August 2023, 43 *Neodon* specimens were collected from Lhozhag County. Integrative genetic and morphological analyses were employed to determine the taxonomic status of these specimens. Results showed distinct morphological and genetic characteristics in the *Neodon* populations from the Lhozhag region, supporting their classification as a new species within the genus. The new species is hereby designated *Neodon lhozhagensis* **sp. nov.** and is formally described below.

MATERIALS AND METHODS

In total, 43 mountain voles were captured from Lhozhag, Xizang, China, during a field survey in August 2023 (Figure 1). Specimens were prepared as skins and skulls, while muscle tissue samples were extracted and preserved in ethanol in the field. These samples were subsequently transferred to a –80°C freezer for storage in the laboratory. All sampling and handling complied with China's regulations for the protection of terrestrial wild animals (State Council Decree (1992) No. 13) and were approved by the Animal Care and Ethics Committee of the Kunming Institute of Zoology (KIZ), Chinese Academy of Sciences (CAS) (SMKX-20191020-212).

Morphological analysis

Morphological analysis was conducted on eight adult specimens of *Neodon lhozhagensis* **sp. nov.** and 113 adult specimens representing 14 additional *Neodon* species (*N. bershulaensis*; *N. bomiensis; N. chayuensis*; *N. clarkei* Hinton, 1923; *N. forresti* Hinton, 1923; *N. irene* Thomas, 1912; *N. leucurus* Blyth, 1863; *N. liaoruii*; *N. linzhiensis*; *N. medogensis*; *N. namchabarwaensis*; *N. sikimensis*; *N. shergylaensis*; and *N. tsonaensis*) (Supplementary Table S2). Adult status was determined based on fully erupted and leveled lower second and third molars. Body weight (BW), head and body length (HB), tail length (TL), hind foot length (HF), and ear length (EL) were taken from specimen tags recorded in the field. Thirteen cranial measurements were taken using digital caliper (0.01 mm precision), following Pan et al. (2007), including condyle basal length (CBL), length of palatal bridge (LPB), length of incisive foramina (LIF), length of upper molars (LUM), maximum outer breadth of the upper molar (BUM), length of auditory bulla (LAB), breadth of auditory bulla (BAB), nasal length (NSL), interorbital breadth (IOB), zygomatic width (ZMW), mastoid width (MTW), braincase height (BCH), and mandibular length (MDL).

Qualitative comparisons of craniodental features were conducted for all available specimens (Supplementary Table S3). Dental abbreviations follow standard conventions, with M for molars, M^x for upper molars, and M_x for lower molars. Dental morphology was observed under a light microscope, with terminology followed Kryštufek & Shenbrot (2022). The number of closed triangles in the first lower molar (M_1) was

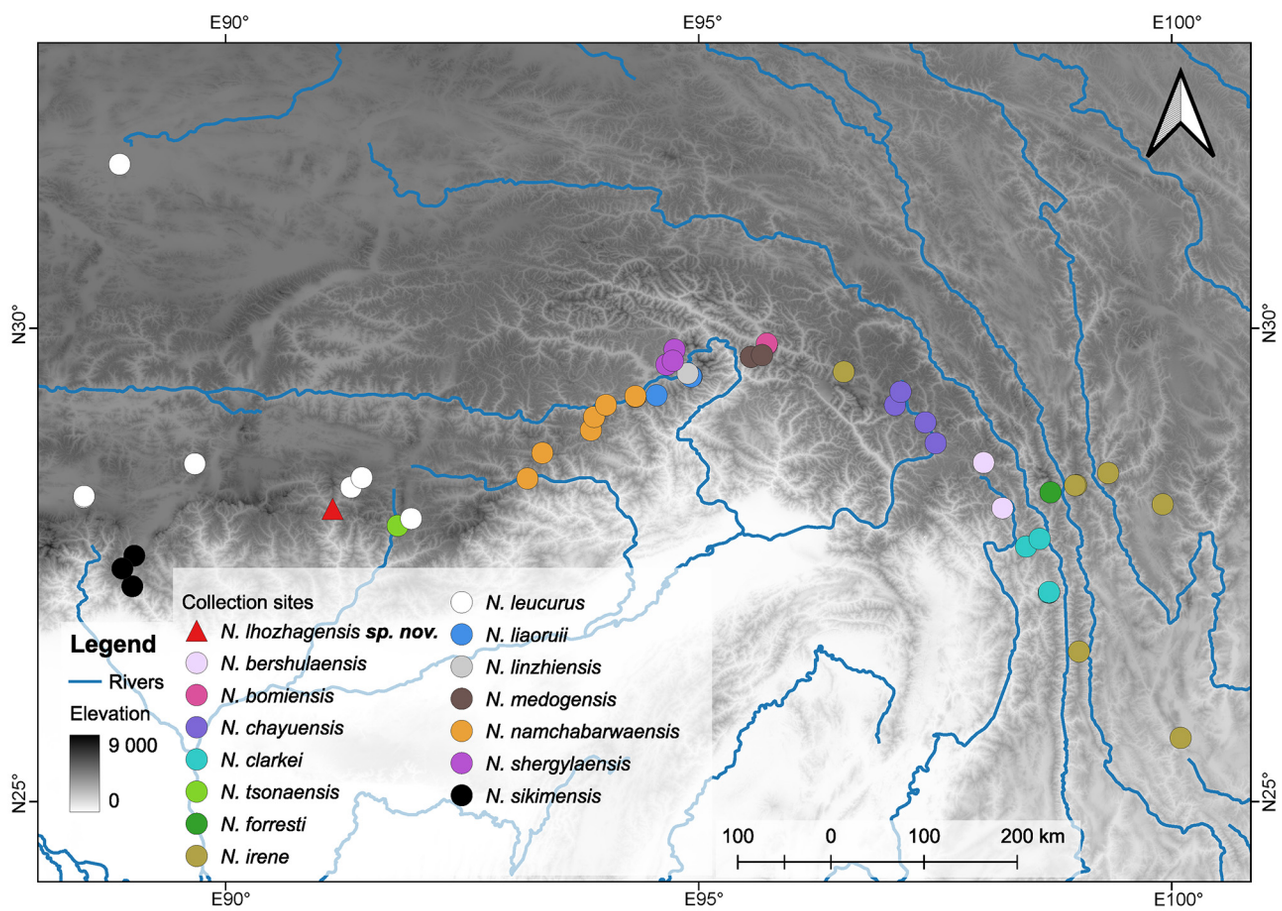

Figure 1 Sample collection localities of specimens used in the present study

documented for all *Neodon* species.

Due to substantial overlap in the principal component analysis (PCA) of the 15 species based on morphological indices, interpretation was challenging (Supplementary Figure S1). Therefore, a separate PCA was performed for *Neodon lhozhagensis* **sp. nov.** and *N. clarkei*, which is the species with the most similar external shape, fur color, and dental characteristics to *Neodon lhozhagensis* **sp. nov.** Kaiser-Meyer-Olkin (KMO) and Bartlett's sphericity tests were used to verify the assumptions of PCA using PAST v.4.10 (Hammer et al., 2001).

Molecular analysis

Molecular data were obtained from six specimens of *Neodon lhozhagensis* **sp. nov.** and 67 specimens representing another 14 known *Neodon* species with preserved muscle tissue (*N. bershulaensis*, *N. bomiensis*, *N. chayuensis*, *N. clarkei*, *N. forresti*, *N. irene*, *N. leucurus*, *N. liaoruii*, *N. linzhiensis*, *N. medogensis*, *N. namchabarwaensis*, *N. shergylaensis*, *N. sikimensis*, and *N. tsonaensis*) (Supplementary Table S4).

Genomic DNA was extracted using a DNeasy Blood and Tissue Kit (Qiagen, Germany) following the manufacturer's instructions. Two mitochondrial genes (cytochrome *b* (*CYTB*, 1131 bp) and cytochrome *c* oxidase subunit 1 (*COI*, 711 bp)) and four nuclear gene fragments (growth hormone receptor gene exon 10 (*GHR*, 504 bp), recombination-activating 1 exon 10 (*RAG1*, 1 074 bp), breast cancer protein 1 exon 11 (*BRCA1*, 831 bp), and retinol-binding protein 3 exon 4 (*IRBP3*, 1 215 bp)), were amplified. These genetic markers, widely employed for phylogenetic reconstruction of *Neodon* (Liu et al., 2017; Pradhan et al., 2019), were purified using a QIAquick PCR Purification Kit (Qiagen, Germany). The primer sequences used for amplification are listed in Supplementary Table S5. The PCR amplicons were sequenced bidirectionally on an ABI 3730 Genetic Analyzer (Applied Biosystems, USA), then assembled and edited using SeqMan in DNASTAR Lasergene v.7.1.0 (Swindell & Plasterer, 1997). Additionally, gene fragments of *N. fuscus* (Buchner, 1889), *N. nepalensis*, *N. nyalamensis*, and two outgroup species, *Alexandromys fortis* (Buchner, 1889) and *Lasiopodomys gregalis* (Pallas, 1779), were downloaded from NCBI GenBank (https://www.ncbi.nlm.nih.gov/genbank) for comprehensive phylogenetic analysis (Supplementary Table S4).

Sequence alignment was performed using MUSCLE (Edgar, 2004) implemented in MEGA X (Kumar et al., 2018). The number of variable and parsimony-informative sites across the six single-gene datasets were calculated using DNA Sequence Polymorphism v.5.1 (Librado & Rozas, 2009). The sequences were concatenated in PhyloSuite v.1.2.3 (Xiang et al., 2023; Zhang et al., 2020) to create two combined datasets: (1) mitochondrial gene dataset (*CYTB*+*COI*) and (2) nuclear gene dataset (*GHR*+*RAG1*+*IRBP3*+*BRCA1*).

Phylogenetic associations were inferred for both datasets using maximum-likelihood (ML) and Bayesian inference (BI) approaches. The optimal evolutionary models for each dataset were selected using ModelFinder v.2.2.0 (Kalyaanamoorthy et al., 2017) (Supplementary Table S6). ML analysis was performed in IQTREE v.2.2.2.6 (Kalyaanamoorthy et al., 2017), with node support estimated using ultrafast bootstrapping approximation (UFBoot) with 5 000 replicates (Guindon et al., 2010; Hoang et al., 2018; Minh et al., 2013). BI analysis was performed in MrBayes v.3.2.6 (Ronquist et al., 2012), employing two independent runs of 2 000 000 generations, with trees sampled every 1 000 generations. The first 25% of sampled trees were discarded as burn-in, and a majority-rule consensus tree was constructed to summarize the results. Effective sample sizes (ESSs) for each estimated parameter were checked in Tracer v.1.7.2, with ESS values exceeding 200 considered sufficient for robust parameter estimation (Rambaut et al., 2018).

Although mitochondrial genes provide valuable information on genetic differentiation among species (Avise, 1986; Ballard & Whitlock, 2004), they are less informative than nuclear genes in reconstructing evolutionary relationships (Edwards et al., 2007; Jarvis et al., 2014). Thus, divergence time were estimated using BEAST v.2.7.4 (Bouckaert et al., 2014) based on the nuclear gene dataset. Two secondary calibration points were incorporated, following Liu et al. (2022): (1) divergence between *Lasiopodomys* Lataste, 1887 and *Neodon*, estimated at 3.4 million years ago (Ma), with a 95% highest posterior density (HPD) interval of 3.0–3.7 Ma, and (2) divergence of the most recent common ancestor of *Neodon*, estimated at 2.3 Ma, with a 95% HPD interval of 2.0–2.6 Ma. The best substitution model and partitioning scheme for analysis were selected using ModelFinder v.2.2.0 (Supplementary Table S6). Divergence time estimation was conducted through 10 independent runs, each initialized with a random starting tree, applying a lognormal relaxed clock model and a birth-death tree prior. For each run, Markov chain Monte Carlo (MCMC) was conducted for 100 million generations, with sampling every 10 000 generations to ensure convergence of the same posterior distribution. Tracer v.1.7.2 was used to assess the stationarity and convergence of parameter estimates, with ESS values greater than 200 interpreted as adequate support (Rambaut et al., 2018). Finally, pairwise Kimura-2-parameter (K2P) distances of *CYTB* were calculated in MEGA X to evaluate the genetic differentiation among species and within *Neodon lhozhagensis* **sp. nov.** (Kimura, 1980; Kumar et al., 2018).

RESULTS

Morphological variation

Our analysis revealed that the number of closed triangles on M_1 within *Neodon* exhibited interspecific variation but remained consistent within a given species. This morphological feature was categorized into three types: (1) three closed triangles, including *N. forresti*, *N. irene, N. leucurus*, *N. liaoruii, N. namchabarwaensis*, *N. nepalensis*, *N. shergylaensis*, *N. sikimensis*, *N. nyalamensis*, and *N. tsonaensis*; (2) four closed triangles, including *N. bomiensis*, *N. chayuensis*, *N. fuscus*, and *N. medogensis*; and (3) five closed triangles, including *N. bershulaensis*, *N. clarkei*, *N. linzhiensis*, and *Neodon lhozhagensis* **sp. nov.** Among adults of the *Neodon* species with five closed triangles on M_1, *N. bershulaensis* can be distinguished by the absence of an interorbital crest, a feature highly prominent in *Neodon lhozhagensis* **sp. nov.**, *N. clarkei*, and *N. linzhiensis*. The TL/HB proportion was also significantly smaller in *N. linzhiensis* (30.00%–35.24%) compared to the other three *Neodon* species (*Neodon lhozhagensis* **sp. nov.** (41.67%–54.17%), *N. bershulaensis* (48.65%–53.28%), and *N. clarkei* (38.10%–51.82%)). Based on these morphological comparisons, all examined *Neodon* species, except for *N. clarkei*, differed significantly from *Neodon lhozhagensis* **sp.**

nov. Subsequent PCA was performed to further differentiate *N. lhozhagensis* **sp. nov.** from *N. clarkei*.

The PCA results yielded a KMO value of 0.725 and a highly significant Bartlett's sphericity test (P<0.001), confirming the suitability of the dataset for PCA. The first three principal components (PC1–3) explained 84.14% of the total variation, each with eigenvalues exceeding 1.0 (Table 1). PC1 explained 60.82% of the total variance and was positively correlated with all measured variables except IOB, indicating that it primarily represented overall skull size. PC2 explained 13.21% of the total variance and was strongly positively correlated with LIF (loading=0.536) and IOB (loading=0.692), highlighting significant differences in these features between the species. PC3 explained 10.12% of the total variance and was strongly positively correlated with BCH (loading=0.773), reflecting variations in cranial height. Scatter plots of PC1 vs. PC2 and PC2 vs. PC3 (Figure 2) revealed clear separation between specimens of *Neodon lhozhagensis* **sp. nov.** and *N. clarkei*. Notably, *Neodon lhozhagensis* **sp. nov.** exhibited a longer incisive foramen (5.4±0.3 mm vs. 4.9±0.4 mm) and broader interorbital breadth (4.2±0.2 mm vs. 4.0±0.1 mm) compared to *N. clarkei* (Supplementary Table S3), underscoring distinct morphological differences between the two species.

Molecular phylogeny

The number of variable and parsimony-informative sites across the genetic datasets is provided in Supplementary Table S7. When using the same dataset, phylogenetic reconstructions using ML and BI approaches produced similar tree topologies, though the construction of the BI trees was significantly superior to that of the ML tree (Figure 3; Supplementary Figures S2, S3). The monophyly of all species was recovered. All six samples from Lhozhag, Xizang formed a monophyletic group with robust support in BI trees. It was resolved as the sister clade to *N. tsonaensis* in the nuclear gene-based phylogeny (Bayesian posterior probability (BPP)=0.99) and as the sister lineage to *N. nepalensis* in the mitochondrial gene-based phylogeny (BPP=0.99). The ML trees also recovered the monophyly of the *Neodon lhozhagensis* **sp. nov.**, but with lower support (Supplementary Figures S2, S3).

Divergence time analysis based on nuclear gene data (Figure 4) estimated that *Neodon lhozhagensis* **sp. nov.** diverged from its sister taxon *N. tsonaensis* approximately 1.28 Ma (95% confidence intervals (CI)=0.89–1.68 Ma), predating the divergence of closely related species pairs within the genus, such as *N. bershulaensis* and *N. clarkei* (0.71 Ma, 95% CI=0.50–0.96 Ma) and *N. bomiensis* and *N. chayuensis* (0.74 Ma, 95% CI=0.50–1.01 Ma).

The interspecific K2P genetic distances within *Neodon* ranged from 3.9% (*N. chayuensis* and *N. bomiensis*) to 13.8% (*N. fuscus* and *N. medogensis*), with an average of 11.2% (Table 2). For *Neodon lhozhagensis* **sp. nov.**, the average K2P genetic distance to the other 17 recognized species was 10.7%, ranging from 9.3% (with *N. liaoruii*) to 12.8% (with *N. fuscus*). In contrast, the genetic divergence among the eight *Neodon lhozhagensis* **sp. nov.** individuals ranged from 0% to 0.74% (average=0.26%) (Supplementary Table S8).

The consistent and highly supported monophyly of *Neodon lhozhagensis* **sp. nov.** in BI trees from both nuclear and mitochondrial datasets, as well as its relatively long divergence time and greater genetic distance than the average interspecific distance within the genus, provides strong evidence for its recognition as a valid species.

Table 1 Principal component analysis showing character loadings, eigenvalues, and percentage variance explained by first three principal components of 13 $\log_{10}$-transformed craniodental measurements of *Neodon clarkei* and *Neodon lhozhagensis* sp. nov.

Character	PC1	PC2	PC3
CBL	0.323	0.131	–0.088
LPB	0.304	0.248	–0.281
LIF	0.230	0.536	–0.023
LUM	0.313	–0.088	–0.283
BUM	0.245	–0.290	0.159
LAB	0.309	–0.033	–0.097
BAB	0.315	–0.012	0.235
NSL	0.323	0.063	–0.133
IOB	–0.054	0.692	0.197
ZMW	0.319	–0.190	0.209
MTW	0.294	–0.110	0.213
BCH	0.065	0.063	0.773
MDL	0.314	–0.072	–0.004
Eigenvalue	7.90604	1.71766	1.31497
% variance	60.816	13.213	10.115

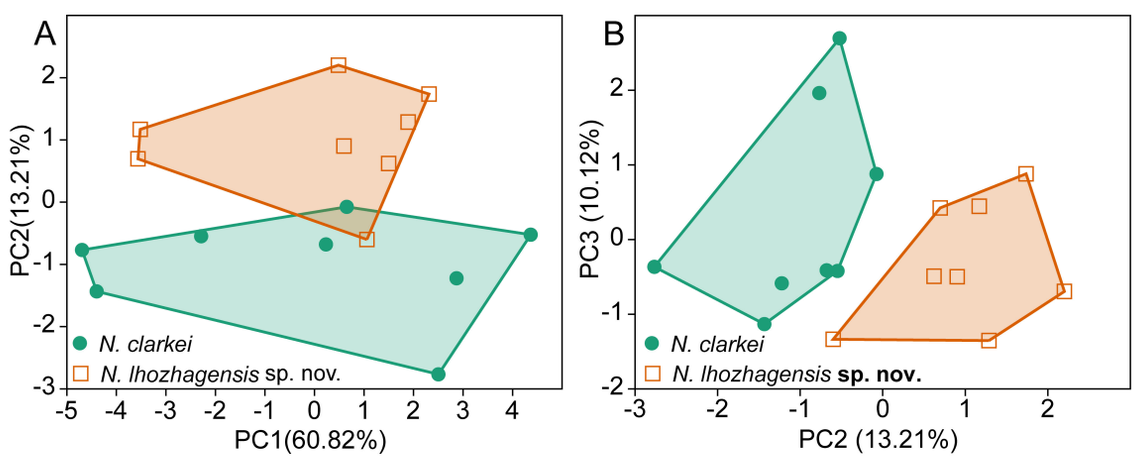

Figure 2 Principal component analysis of *Neodon lhozhagensis* sp. nov. and *N. clarkei* based on 13 $\log_{10}$-transformed craniodental measurements

A: Scatterplot of PC1 vs. PC2. B: Scatterplot of PC2 vs. PC3. Node labels represent posterior probabilities.

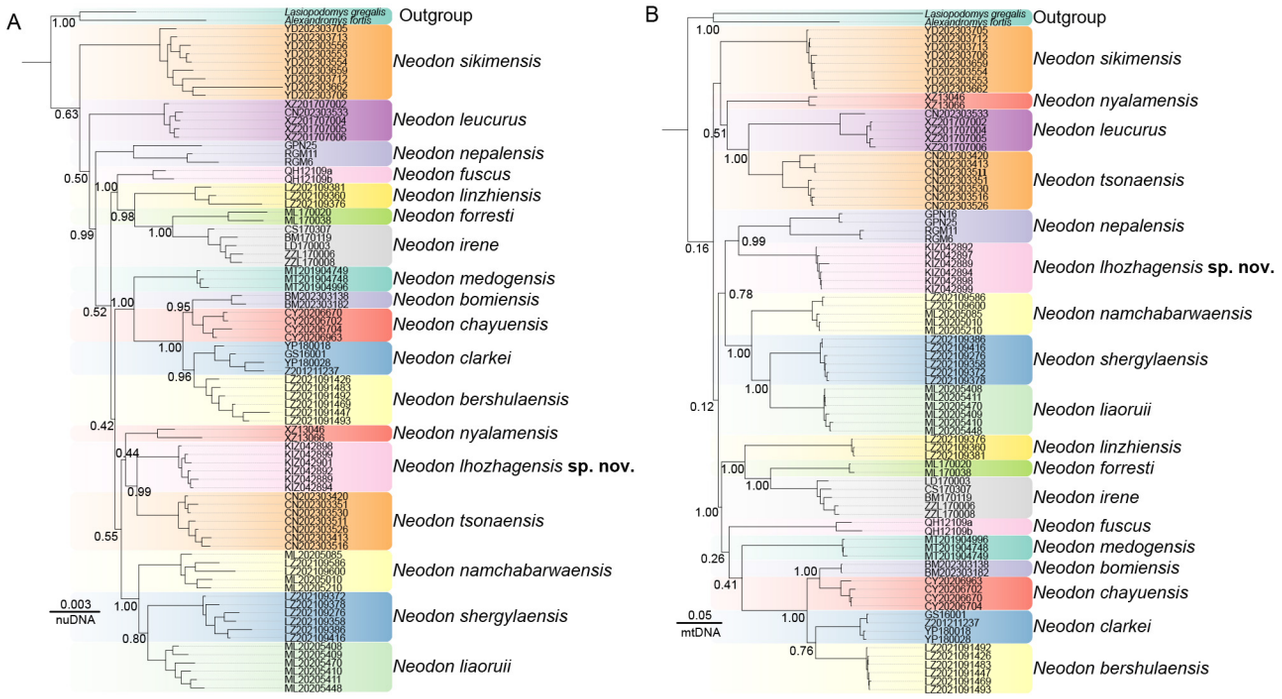

Figure 3 Phylogenetic tree of *Neodon* constructed using Bayesian inference based on (A) nuclear and (B) mitochondrial gene datasets

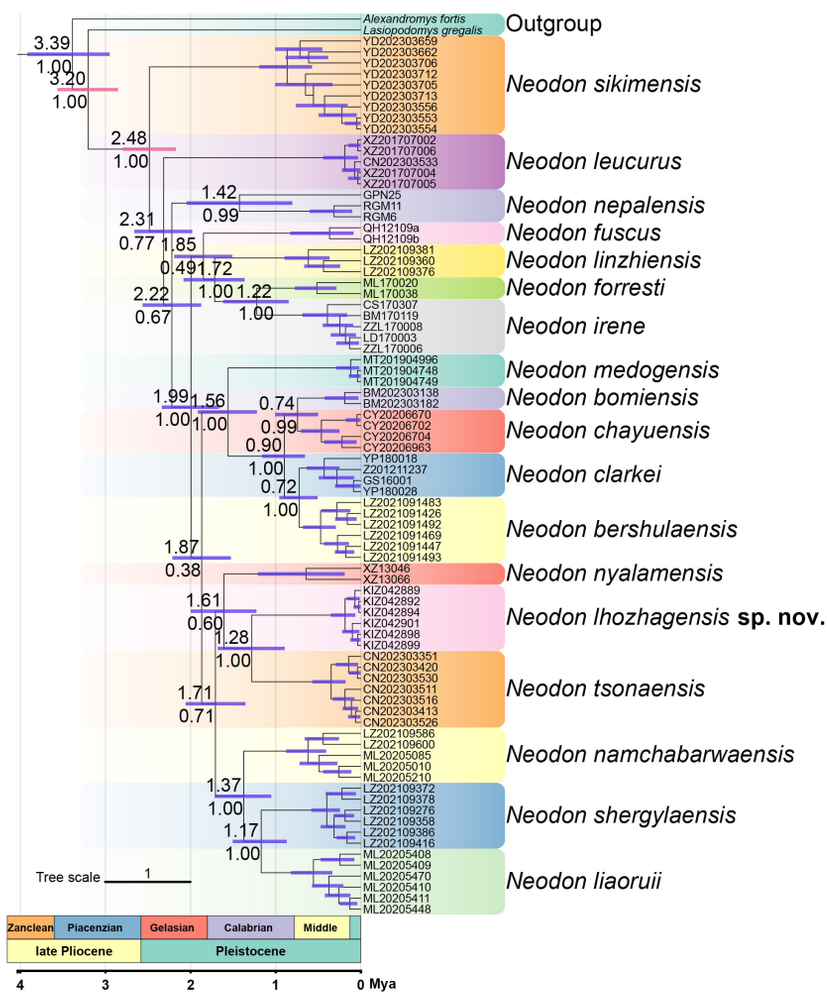

Figure 4 Phylogenetic tree and divergence estimates of *Neodon* based on four nuclear genes in BEAST v.2.7.4

Branch lengths represent time. Node labels represent divergence time (above) and posterior probabilities (below). Blue node bars represent 95% confidence intervals of divergence time, and red bars indicate calibration points.

Table 2 Estimates of evolutionary divergence between *Neodon* species based on *CYTB* using Kimura 2-parameter model

	1	2	3	4	5	6	7	8	9	10	11	12	13	14	15	16	17
1. *lhozhagensis* **sp. nov.**																	
2. *irene*	0.103																
3. *bomiensis*	0.104	0.114															
4. *tsonaensis*	0.095	0.115	0.089														
5. *leucurus*	0.112	0.114	0.123	0.101													
6. *chayuensis*	0.115	0.122	0.039	0.098	0.126												
7. *nepalensis*	0.109	0.124	0.130	0.115	0.128	0.135											
8. *clarkei*	0.113	0.127	0.061	0.098	0.125	0.065	0.136										
9. *bershulaensis*	0.114	0.120	0.061	0.099	0.128	0.069	0.134	0.069									
10. *shergylaensis*	0.099	0.114	0.107	0.089	0.110	0.114	0.123	0.119	0.119								
11. *linzhiensis*	0.117	0.112	0.127	0.123	0.134	0.131	0.134	0.127	0.132	0.123							
12. *namchabarwaensis*	0.094	0.107	0.097	0.095	0.114	0.108	0.128	0.108	0.109	0.085	0.115						
13. *forresti*	0.106	0.087	0.113	0.112	0.123	0.126	0.131	0.122	0.123	0.115	0.114	0.110					
14. *liaoruii*	0.093	0.111	0.101	0.087	0.113	0.106	0.117	0.107	0.106	0.070	0.125	0.076	0.110				
15. *medogensis*	0.111	0.118	0.103	0.116	0.132	0.113	0.125	0.110	0.120	0.109	0.123	0.105	0.116	0.099			
16. *fuscus*	0.128	0.128	0.119	0.117	0.129	0.135	0.137	0.122	0.131	0.131	0.132	0.135	0.126	0.121	0.138		
17. *nyalamensis*	0.110	0.110	0.103	0.091	0.120	0.113	0.131	0.114	0.110	0.109	0.122	0.101	0.107	0.102	0.125	0.131	
18. *sikimensis*	0.099	0.106	0.091	0.094	0.107	0.098	0.120	0.102	0.111	0.114	0.112	0.098	0.107	0.105	0.124	0.117	0.092

Combined with its unique morphological characteristics and allopatric distribution with other *Neodon* species, *Neodon lhozhagensis* **sp. nov.** is formally described below.

TAXONOMIC ACCOUNT

***Neodon lhozhagensis* Wang & Jiang, sp. nov.**

Suggested common name: Lhozhag mountain vole, 洛扎松田鼠.

Holotype: KIZ042896 (Field number SN202308716), adult female collected on 28 August 2023 by Mr. Luo Kang from Lakang Township, Lhozhag County, south Xizang, China (N28.104°, E91.139°, 3729 m above sea level (a.s.l.)). The dried skin, cleaned skull, and ethanol-preserved body are deposited in the Kunming Natural History Museum of Zoology, Kunming Institute of Zoology, Chinese Academy of Sciences.

Paratypes: Seven adult specimens, collected from the type locality in August 2023: KIZ042890 (Field number SN202308670, adult female), KIZ042891 (Field number SN202308654, adult male), KIZ042893 (Field number SN202308680, adult female), KIZ042895 (Field number SN202308703, adult male), KIZ042897 (Field number SN202308749, adult male), KIZ042932 (Field number SN202308785, adult male), and KIZ042933 (Field number SN202308798, adult female). Dry skins and clean skulls are deposited in the Kunming Natural History Museum of Zoology, Kunming Institute of Zoology, Chinese Academy of Sciences.

Etymology: The specific name *lhozhag* is derived from Lhozhag County, the type locality of the new species, and *–ensis* is Latin for “belonging to”.

Distribution: The Lhozhag mountain vole is presently known only from Lhozhag County, south Xizang, China, at elevations of 2800–4000 m a.s.l. It is allopatric with other *Neodon* species.

Habitat: Bamboo forests, coniferous forests, and shrubs.

Diagnosis: The M_1 of *Neodon lhozhagensis* **sp. nov.** possesses five closed triangles anterior to the posterior transverse space, a characteristic shared with *N. clarkei*, *N. bershulaensis*, and *N. linzhiensis*, but distinct from all other known species of the genus. The interorbital crest is prominently developed, differentiating it from *N. bershulaensis* (Figure 5). Compared to *N. clarkei*, *Neodon lhozhagensis* **sp. nov.** has a longer incisive foramina (5.4±0.3 mm vs. 4.9±0.4 mm) and a wider interorbital breadth (4.2±0.2 mm vs. 4.0±0.1 mm). Additionally, the new species is characterized by a larger body size, including a longer tail and a greater relative tail length (TL=50–65 mm; TL/HB=41.67%–54.17%) compared to *N. linzhiensis* (TL=27–37 mm; TL/HB=30.00%–35.24%).

Description: Large mountain vole. Head-body length 110–130 mm (average 118.8 mm), tail length 50–65 mm (average 56.8 mm), and large relative tail/head and body length 41.67%–54.17% (average 47.9%). Dorsal pelage deep brownish-black, interspersed with yellow to dark ferruginous-brown hair tips. Ventral pelage blackish slate tipped and white, boundary between back and abdomen not obvious. Tail visibly bicolored, dorsal dark brown, ventral grayish white. Tip of tail with elongated dense hairs. Ears project slightly above pelage, covered with dense dark-brown hairs. Limbs covered with short hair, lighter in color than ventral pelage, and claws hook-like.

Skull robust, with strong and angular zygomatic arches, short and slender rostrum, and large octagonal shaped brain case. Nasals anteriorly broad and posteriorly narrow. Zygomatic arches moderately expanded. Orbits large, interorbital breadth narrow (IOB=3.92–4.40 mm), especially at posterior. Anterior edge of squamosa possesses angular projection, contributing to octagonal appearance of brain case. Temporal ridges very distinct, fused to form apparent midline ridge in interorbital region (Figure 5).

Interparietal bone large and wide. Incisive foramina long, thin, and posteriorly constricted. Pterygoid region narrow, with relatively square shape in anterior view. Auditory bullae large and inflated (LAB=6.5–7.29 mm; BAB=5.88–6.33 mm). Foramen magnum large. Mandible stout (LLM=6.18–7.17 mm). Coronoid process slender, with posteriorly pointing tip, sitting well forward and just below condyle. Condyloid process large, high, thick, and rectangular; condyle positioned far above toothrow. Angular process long and slender, pointing upward (Figure 6).

Upper incisors orange. M^1 possesses three closed triangles after anterior transverse space, forming three inner angles and three outer angles. M^2 contains two closed triangles after

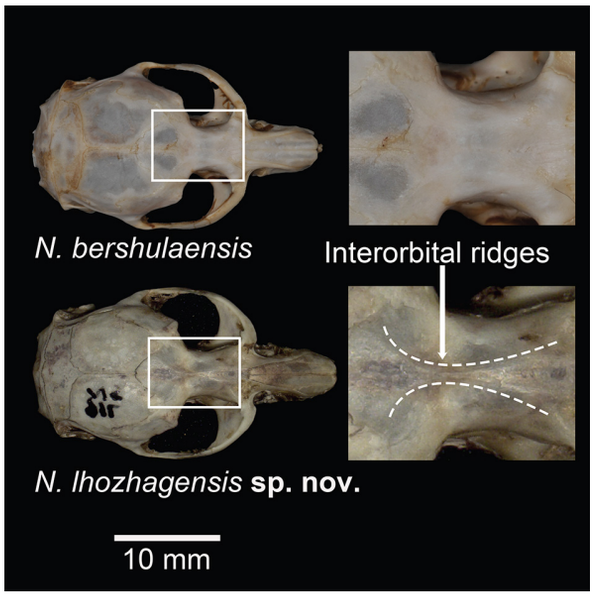

Figure 5 Comparison of interorbital regions of *N. bershulaensis* (upper) and *Neodon lhozhagensis* sp. nov. (lower)
Photo by S.Y.W.

Figure 6 Skull and skin of *Neodon lhozhagensis* sp. nov. (KIZ042896)
A: Dorsal, ventral and lateral views of skull and mandibles; B: Upper and lower molars; C: Dorsal, ventral, and lateral views of skin. Scale bars: 10 mm (A); 2 mm (B); 50 mm (C). Photo by S.Y.W.

anterior transverse space, forming three inner and three outer angles. M^3 contains three closed triangles, forming four inner and three outer angles. M_1 contains five closed triangles anterior to posterior transverse space and trefoil anterior tooth cap. Most specimens (63.6%) exhibited six inner and four outer angles, with 36.4% having six inner and five outer angles. M_2 and M_3 both show three outer and three inner angles.

Comparison: *Neodon lhozhagensis* **sp. nov.** can be distinguished from all known *Neodon* species by the following combination of characteristics: Five closed triangles in M_1 (vs. three or four closed triangles in *N. leucurus*, *N. forresti*, *N. irene*, *N. nepalensis*, *N. liaoruii*, *N. namchabarwaensis*, *N. shergylaensis*, *N. sikimensis*, *N. nyalamensis*, *N. tsonaensis*, *N. fuscus*, *N. bomiensis*, *N. chayuensis*, and *N. medogensis*). Of the four species of *Neodon* with five closed triangles in M_1, *Neodon lhozhagensis* **sp. nov.** can be distinguished from *N. bershulaensis* by interorbital crest present (vs. absent); from *N. linzhiensis* by larger body size (HB=110–130 mm, TL=50–65 mm) and greater TL/HB proportion (41.7%–54.2%) (vs.HB=90–105 mm, TL=27–37 mm, and TL/HB=30.0%–35.2%); and from *N. clarkei* by longer incisive foramina (5.4±0.3 mm) and wider interorbital breadths (4.2±0.2 mm) (vs. LIF=4.9±0.4 mm, IOB=4.0±0.1 mm).

DISCUSSION

The genus *Neodon* is endemic to the Qinghai-Xizang Plateau and its surrounding high-altitude mountains. Historically, *Neodon* was thought to comprise only four species, with a series of junior synonyms (Musser & Carleton, 2005). However, advancements in molecular phylogenetic techniques and the expansion of survey efforts have significantly reshaped this understanding. Over the past decade, nine new species have been described, and the taxonomic status of some existing species has been revised, bringing the current total to 17 recognized species (Liu et al., 2022; Liu, 2024; Pradhan et al., 2019). The rapid increase in the number of species highlights the remarkable diversity of *Neodon* in the Himalayas and Hengduan Mountains, where several species exhibit restricted distribution ranges (Liu et al., 2022). These findings underscore the need for more comprehensive and systematic surveys in these regions.

Despite this progress, some areas in south Xizang, such as Lhozhag, remain underexplored. Our recent field survey in Lhozhag, combined with subsequent morphological and molecular analyses, led to the identification of a new species. This discovery suggests that additional species of *Neodon* are likely to be uncovered in the Himalayas and Hengduan Mountains through further targeted fieldwork and systematic investigations.

This study also identified a notable incongruence between mitochondrial and nuclear gene phylogenies, consistent with observation by Liu et al. (2022). Such topological inconsistencies may reflect complex evolutionary histories, including hybridization, incomplete lineage sorting, or differential rates of molecular evolution (Duan et al. 2023). Future analyses using genome-wide data are essential to resolve these discrepancies and to elucidate the processes driving the dispersal, diversification, and rapid speciation of *Neodon* in the Qinghai-Xizang Plateau and adjacent montane regions.

NOMENCLATURAL ACTS REGISTRATION

This study and the nomenclatural act it contains are registered with ZooBank, the official registry of the International Code of Zoological Nomenclature (ICZN). Publication ID: http://zoobank.org/CF924F18-E32D-4428-A7D6-285FE767FE93.

SCIENTIFIC FIELD SURVEY PERMISSION INFORMATION

Fieldwork was conducted with the permission of Xizang Autonomous Region Forestry and Grassland Bureau ((2023) No. 22).

DATA AVAILABILITY

Mitochondrial and nuclear sequence datasets have been deposited to Genbank under the accession numbers PQ382935–PQ383268; PQ410346–PQ410415 and Science Data Bank (https://www.scidb.cn/) under DOI: 10.57760/sciencedb.zrdc.00010.

SUPPLEMENTARY DATA

Supplementary data to this article can be found online.

CONFLICT OF INTEREST

The authors declare that they have no competing interests.

AUTHORS' CONTRIBUTIONS

X.L.J. conceived the research; Q.L. and W.Y.S. collected the specimens and samples; S.Y.W., Y.X.L., H.J.W., and S.W.H. conducted the lab work; S.Y.W., Y.X.L., Q.L., Z.Z.C., and X.Y.L. analyzed the data; S.Y.W. and Y.X.L. wrote the manuscript; Z.Z.C., Q.L., W.Y.S., X.Y.L., K.O.O., L.K., and X.L.J. revised and X.L.J. finalized the manuscript. All authors read and approved the final version of the manuscript.

ACKNOWLEDGMENTS

We thank Changzhe Pu, Jing Luo, Kang Luo, and Mingjing Pu for specimen and tissue collection, and the Xizang Forestry and Grassland Administration for permits and logistical support. We gratefully acknowledge Kunming Natural History Museum of Zoology for assistance in specimen examination.

REFERENCES

Avise JC. 1986. Mitochondrial DNA and the evolutionary genetics of higher animals. *Philosophical Transactions of the Royal Society B: Biological Sciences*, **312**(1154): 325–342.

Ballard JWO, Whitlock MC. 2004. The incomplete natural history of mitochondria. *Molecular Ecology*, **13**(4): 729–744.

Bouckaert R, Heled J, Kühnert D, et al. 2014. BEAST 2: a software platform for Bayesian evolutionary analysis. *PLoS Computational Biology*, **10**(4): e1003537.

Corbet GB. 1978. The Mammals of the Palaearctic Region: A Taxonomic Review. London: British Museum.

Duan L, Fu L, Chen HF. 2023. Phylogenomic cytonuclear discordance and evolutionary histories of plants and animals. *Science China Life Sciences*, **66**(12): 2946–2948.

Edgar RC. 2004. MUSCLE: multiple sequence alignment with high accuracy and high throughput. *Nucleic Acids Research*, **32**(5): 1792–1797.

Ellerman, JR. 1941. The Families and Genera of Living Rodents. British Museum of Natural History. London: Printed by Order of the Trustees of the British Museum, 1–642.

Edwards SV, Liu L, Pearl DK. 2007. High-resolution species trees without concatenation. *Proceedings of the National Academy of Sciences of the United States of America*, **104**(14): 5936–5941.

Guindon S, Dufayard JF, Lefort V, et al. 2010. New algorithms and methods to estimate maximum-likelihood phylogenies: assessing the performance of PhyML 3.0. *Systematic Biology*, **59**(3): 307–321.

Hammer Ø, Harper DAT, Ryan PD. 2001. PAST: paleontological statistics software package for education and data analysis. *Palaeontologia Electronica*, **4**(1): 9.

Hinton MAC. 1923. XII. —On the voles collected by Mr. G. Forrest in Yunnan; with remarks upon the genera *Eothenomys* and *Neodon* and upon their allies. *Annals and Magazine of Natural History*, **11**(61): 145–162.

Hinton MAC. 1926. Monograph of the Voles & Lemmings (Microtinae) Living and Extinct. London: Printed by Order of the Trustees of the British Museum, 1–475.

Hoang DT, Chernomor O, Von Haeseler A, et al. 2018. UFBoot2: improving the ultrafast bootstrap approximation. *Molecular Biology and Evolution*, **35**(2): 518–522.

Horsfield T. 1851. A Catalogue of the Mammalia in the Museum of the Hon. East-India Company. London: Printed by J. & H. Cox.

Jarvis ED, Mirarab S, Aberer AJ, et al. 2014. Whole-genome analyses resolve early branches in the tree of life of modern birds. *Science*, **346**(6215): 1320–1331.

Kalyaanamoorthy S, Minh BQ, Wong TKF, et al. 2017. ModelFinder: fast model selection for accurate phylogenetic estimates. *Nature Methods*, **14**(6): 587–589.

Kimura M. 1980. A simple method for estimating evolutionary rates of base substitutions through comparative studies of nucleotide sequences. *Journal of Molecular Evolution*, **16**(2): 111–120.

Kryštufek B, Shenbrot G. 2022. Voles and Lemmings (Arvicolinae) of the Palaearctic Region. Maribor: University of Maribor, 219–238.

Kumar S, Stecher G, Li M, et al. 2018. MEGA X: molecular evolutionary genetics analysis across computing platforms. *Molecular Biology and Evolution*, **35**(6): 1547–1549.

Librado P, Rozas J. 2009. DnaSP v5: a software for comprehensive analysis of DNA polymorphism data. *Bioinformatics*, **25**(11): 1451–1452.

Liu ES. 2024. Morphological and Molecular Phylogenetic Studies on A New Species of Rodent (*Neodon tsonaensis*), and A New Record (*Niviventer gladiusmaculus*), in Southern Xizang. Master thesis, Guizhou Normal University, Guiyang.

Liu SY, Jin W, Liu Y, et al. 2017. Taxonomic position of Chinese voles of the tribe Arvicolini and the description of 2 new species from Xizang, China. *Journal of Mammalogy*, **98**(1): 166–182.

Liu SY, Sun ZY, Liu Y, et al. 2012. A new vole from Xizang, China and the molecular phylogeny of the genus *Neodon* (Cricetidae: Arvicolinae). *Zootaxa*, **3235**: 1–22.

Liu SY, Zhou CR, Meng GL, et al. 2022. Evolution and diversification of Mountain voles (Rodentia: Cricetidae). *Communications Biology*, **5**(1): 1417.

Minh BQ, Nguyen Mat, Von Haeseler A. 2013. Ultrafast approximation for phylogenetic bootstrap. *Molecular Biology and Evolution*, **30**(5): 1188–1195.

Musser GG, Carleton MD. 1993. Family muridae. *In*: Wilson DE, Reeder DM. Mammal Species of the World. 2nd ed. Washington: Smithsonian Institution, 501–535.

Musser GG, Carleton MD. 2005. Superfamily muroidea. *In*: Wilson DE, Reeder DM. Mammal Species of the World. 3rd ed. Baltimore: The Johns Hopkins University Press, 958–1039.

Pan QH, Wang YX, Yan K. 2007. A Field Guide to the Mammals of China. Beijing: China Forestry Publishing House.

Pradhan N, Sharma AN, Sherchan AM, et al. 2019. Further assessment of the Genus *Neodon* and the description of a new species from Nepal. *PLoS One*, **14**(7): e0219157.

Rambaut A, Drummond AJ, Xie D, et al. 2018. Posterior summarization in Bayesian phylogenetics using Tracer 1.7. *Systematic Biology*, **67**(5): 901–904.

Ronquist F, Teslenko M, Van Der Mark P, et al. 2012. MrBayes 3.2: efficient Bayesian phylogenetic inference and model choice across a large model space. *Systematic Biology*, **61**(3): 539–542.

Swindell SR, Plasterer TN. 1997. SEQMAN: contig assembly. *In*: Swindell SR. Sequence Data Analysis Guidebook. Totowa: Humana, 75–89.

Thomas O. 1912. The duke of bedford's zoological exploration of Eastern Asia. —XV. On Mammals from the Provinces of Szechwan and Yunnah, Western China. *Proceedings of the Zoological Society of London*, **82**(1): 127–141.

Xiang CY, Gao FL, Jakovlić I, et al. 2023. Using PhyloSuite for molecular phylogeny and tree-based analyses. *iMeta*, **2**(1): e87.

Zhang D, Gao FL, Jakovlić I, et al. 2020. PhyloSuite: an integrated and scalable desktop platform for streamlined molecular sequence data management and evolutionary phylogenetics studies. *Molecular Ecology Resources*, **20**(1): 348–355.